A Search for Astrophysical Gravitational Waves Using LIGO S6 Data

Dylan Langone

1. Abstract

While previous searches of the LIGO S6 data run have thus far failed to identify astrophysical sources of gravitational waves, namely compact binary coalescences or CBC's, the advent of novel numerical relativity templates in the years since the data run's end in October 2010 heightens the prospects of detection. A three phase search method is employed to achieve search efficiency due to time and memory constraints. The first, bandpass filtering, reduces the size of the raw strain data to be analyzed by restricting its frequencies to those that are less than or equal to the template power at those frequencies. The result is passed to time domain cross-correlation, finds the time in which the template most closely resembles the bandpassed strain. Finally, matched filtering finds the signal-to-noise ratio between the template and the strain. The times at which the SNR is greater than 8 is recorded and overlapping times between the two LIGO detectors are found and the raw strain is examined to find a matching signal in both detectors. Despite almost 500 overlapping SNRs and tens of thousands of unique high SNRs, no candidate was deemed worthy of further consideration due to a lack of similarity between the two strains at those times. False detection alarms may be due to other wave sources that the templates happen to model well in some portion of their domains. A more comprehensive search should be conducted in the future with more lenient time and memory constraints to analyze the remainder of the data and templates. More advanced detectors should also allow for the detection of a more diverse array of astrophysical sources.

2. Introduction

Gravitational Waves are disturbance phenomena that transport gravitational energy through space-time. These waves are generated by massive celestial bodies, such as binary star systems, black holes, and neutron stars as they spin and interact with other massive bodies. Originally predicted by Albert Einstein in his theory of general relativity, these waves fit neatly into the new paradigm that gravitational forces are caused by the curvature of space-time. The effect of gravitational waves is the propagation of distortions of the space-time fabric, which is analogous

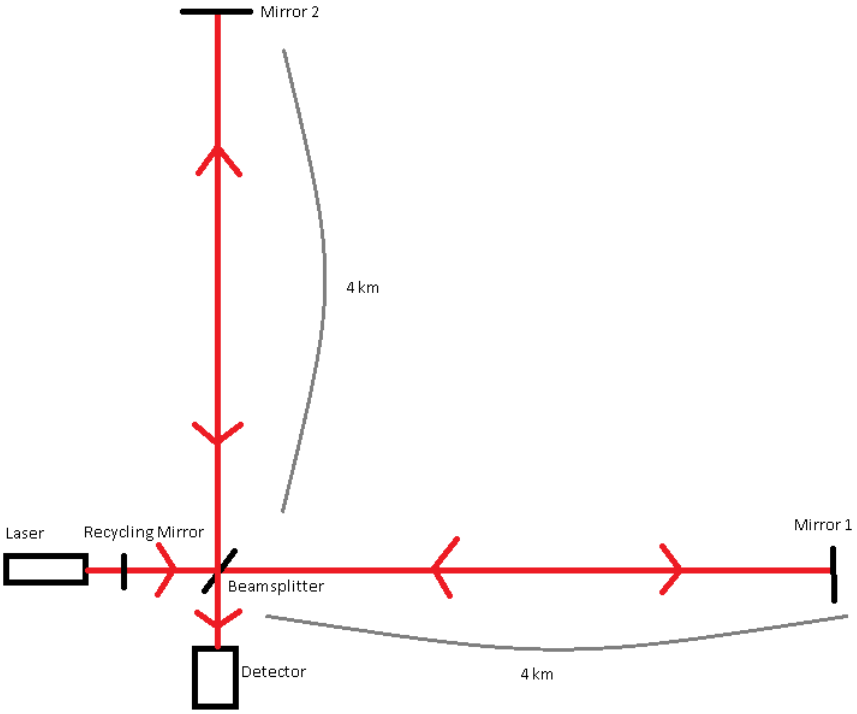

Figure 1: A laser beam originates at a source. Then, it travels through one end of a recycling mirror that does not have a significant effect on the intensity of the beam as it passes through it from the left. When the beam reaches the beamsplitter, it diverges into two beams of roughly equal intensity. The two beams travel down the arms, which are not to scale, and at the end of which the beams encounter a mirror in each arm. This reflects the beams back towards the beamsplitter where some photons from Mirror 1 pass straight though the beamsplitter to be reflected by the Recycling Mirror, allowing for less laser output from the source, and others are reflected and hit the detector. Photons reflecting off of Mirror 2 either pass straight through the beamsplitter and hit the detector or are reflected by the beamsplitter and are reflected once again by the Recycling Mirror.

to the propagation of distortions on the surface of a pond caused by a rock that has been thrown in.

As with other aspects of Einstein's theory of gravity, theoretical predictions such as gravitational waves were not experimentally observed until decades later. Black holes, for instance, were not discovered by astronomers until the 1960's, half a century after the theory of general relativity was published. The wait for the observation of gravitational waves has gone on into the 21st century, with the first discovery taking place in September of 2015 at the Advanced Laser Interferometer Gravitational-Wave Observatory, or LIGO [1]. This first detection of gravitational waves was the culmination of a 40 year search process that began in the 1970's. The first instruments for detection were large aluminum bars that would periodically expand and contract should a gravitational wave influence it. Until the late 1980's the bar implementation was thought to have the largest frequency band for detection. When improvements in interferometer technology came about in the early 1990's, the largest detectable frequency bands were firmly in the hands of large-scale interferometers. In that decade the National Science Foundation approved funding for its most financially ambitious project in its history, LIGO. The experiment is large scale, as two detector sites in Livingston, Louisiana and Hanford, Washington each have two L-shaped interferometer arms of a length of 4 km. The LIGO interferometer setup detects gravitational waves by measuring small deviations in the laser interference pattern caused by the distortion of space-time by the wave. Since the arms of the detector are perpendicular, if the gravitational wave causes one arm to expand slightly, the other arm will contract, and a measureable phase difference may be observed due to the slight variations in the distances of each arm [2]. Figure 1 displays the setup in more detail. This phase difference results in a calculable difference is the length of the detector arms should the phase difference be the result of a gravitational wave phenomenon. The LIGO Open Science Center releases data on this variation in detector arm length in terms of length variation from the original length versus time, known as the strain. For a gravitational wave caused by a compact binary coalescence (CBC) of black holes, the strain appears in a pattern similar to the one in Figure 2. This plot was made from a CBC template that models the gravitational wave signal that LIGO would observe. Such templates are employed to search for gravitational wave signals.

LIGO ran six science data runs from 2002 to 2010. Each successive run was more sensitive than the last, as modest improvements were made in detector equipment in the time between runs. The most sensitive run was the S6 data run, with a measureable frequency range

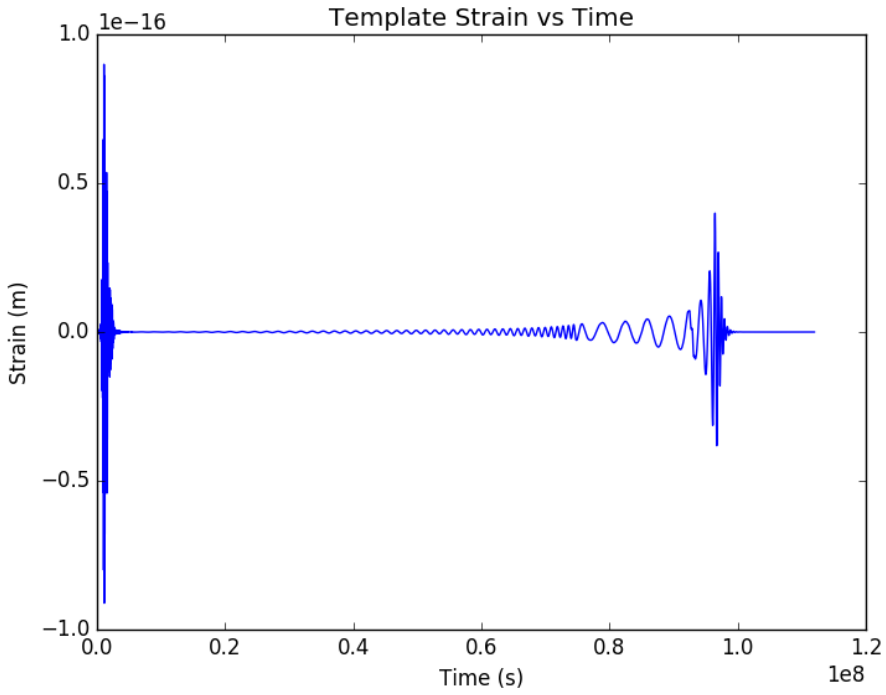

Figure 2: A plot of the hypothetical strain versus time for a CBC of black holes

between 20 Hz and 7,000 Hz [3]. Astrophysical sources of gravitational waves would be detectable by an experiment such as LIGO if the waves the generated waves fall within a certain frequency range, known as the detector sensitivity, and fit a known waveform for that source. One such source would be the stochastic gravitational wave background, which consists of redshifted gravitational waves generated during the big bang. This source is analogous to the cosmic microwave background radiation first detected in the 1960's, giving evidence in favor of the big bang model of cosmology. The stochastic background frequency range is expected to be much lower than what is currently detectable with any gravitational wave detector yet developed. In what would likely be a spectacular gravitational wave event, the gravitational collapse of a star undergoing a supernova would generate a waveform whose profile is still unknown due to the complexity of the internal structure of the collapse. Thus, if such an event were observed, it would not be recognizable because its waveform is currently unknown [2]. That leaves two major sources: black hole and neutron star normal modes, and black hole CBC's. The first, normal mode gravitational waves, is caused by the rotation of such bodies. Each rotating body emits gravitational waves uniformly with a frequency most strongly related to that body's natural frequency f_0, which is given by [4]:

$$f_0 = \sqrt{\frac{G\bar{p}}{4\pi}} \qquad (1)$$

Where,

$$\bar{p} = \frac{3M}{4\pi R^2}$$

$M$is the mass of the body, R is its radius, and $\bar{p}$ is known as the mass-energy density of the body. For black holes the range of masses detectable with LIGO S6 is calculated in the Results section and Figure 3.

How many CBC's occur within LIGO's range of detection and how many of these detections should LIGO detect? The distance range over which the LIGO S6 configuration is able to detect CBC's spans a radius of 160 million light-years [5], which contains the entire Virgo Supercluster. Within just the Milky Way Galaxy, there is one neutron star CBC every 10^5years [2]. There are 10^8 stars in the Milky Way and 10^{21} stars in the observable universe [6]. From this it would be expected that there are 10^{21}x $\frac{10^{-5}}{10^8} = 10^8$coalescences per year in the observable universe, which spans a radius of 46.5 billion light years. The volume of LIGO S6's detectable range is $4.07x10^{-14}$ that of the observable universe. Assuming that galaxies and their stars are roughly uniformly distributed throughout the observable universe, a rate of about $4x10^{-6}$ coalescences per year within LIGO's detectable range would be expected. This figure accounts only for binary neutron star coalescences and does not include binary black hole coalescences. The LIGO Scientific Collaboration estimated that for the S5 data collection run the number of detections should be about .02 detections per year, with a range between .0002 and .2 detections per year [7]. This figure should be higher due to the fact that numerical relativity templates that model CBC's have increased in number and scope since the end of the S6 data run [8].

3. Materials and Methods

In order to detect astrophysical gravitational waves, a common signal processing algorithm known as matched filtering is employed. The goal of the procedure is to recover a known signal represented by a filter from a noisy signal polluted by external and perhaps random signals. In the case of the LIGO detectors, the known signal to be recovered is the signal produced by the

gravitational wave, and the undesirable noise is caused by random fluctuations in the structure and positions of the mirrors caused by quantum noise and environmental factors. These environmental factors include seismic waves, atmospheric pressure variations, and even ground vibrations caused by passing traffic.

Matched filtering against the LIGO S6 data is used to produce an empirical signal to noise ratio (SNR). The SNR is defined as the ratio of the power of the expected signal contained in the noise to the remainder of the total signal or the "noisy" part of the total signal. A high SNR indicates that the signal from an incident gravitational wave is strong compared to the random noise that the detector produces. It is difficult to identify even a strong gravitational wave signal due to the presence of such noise. To confirm the detection of a gravitational wave, the same or a very similar signal must be observed in both LIGO detectors.

The search process presents the challenge of efficiency. A comprehensive search requires that hundreds of templates are used to calculate SNRs for over a year of data for two detectors. The public database contains over three hundred unique CBC templates. Each one must be individually matched to about two terabytes of data recorded for the S6 run. Hence matched filtering is an arduous process, and efficiency is a top priority in conducting the analysis.

The SNR is calculated using the method described below for segments of LIGO data each 2048 seconds long. This limit is imposed to prevent the computer performing the computations from running out of memory. A list of SNR values over eight is generated and another list at which those SNR values occur in each detector is generated as well. The time lists between the two detectors are compared and should any overlapping times be found, then a visual signal examination is conducted at those times. Should a signal be detected, the time at which both detectors observe the signal will not be exactly the same because gravitational waves travel at the speed of light. Therefore, there is a window of .00972 seconds that is allowed between high SNR readings for signals to be directly compared, since this is the time it takes for light to travel from one detector to the other. Only times of high SNR values on different detectors that occur within .00972 seconds of each other are considered to be candidates for a gravitational wave signal. The following flowchart outlines the steps used to calculate SNRs and match the times.

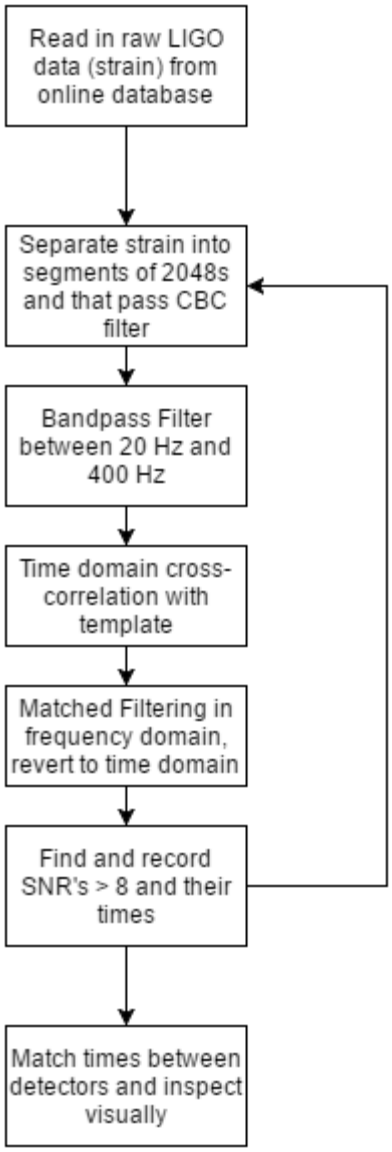

Figure 3: A flowchart for the main analysis procedure

The database files are large, as they usually take up 128 megabytes of space for every 4096 seconds, or just over an hour. Files are loaded into the analysis program one at a time and are then halved to a prevent memory overload. Then the data is filtered down into just segments that are suitable for CBC analysis, which is specified by a python dictionary contained in every data file. This lessens the burden of data that must be analyzed and increases computational efficiency. The third step is to apply a bandpass filter to the CBC data. This decreases the amount of data to be analyzed further by constraining the data to that which passes through a specified frequency window, which in the case shown below in Figure 4, is between 20 Hz and 250 Hz.

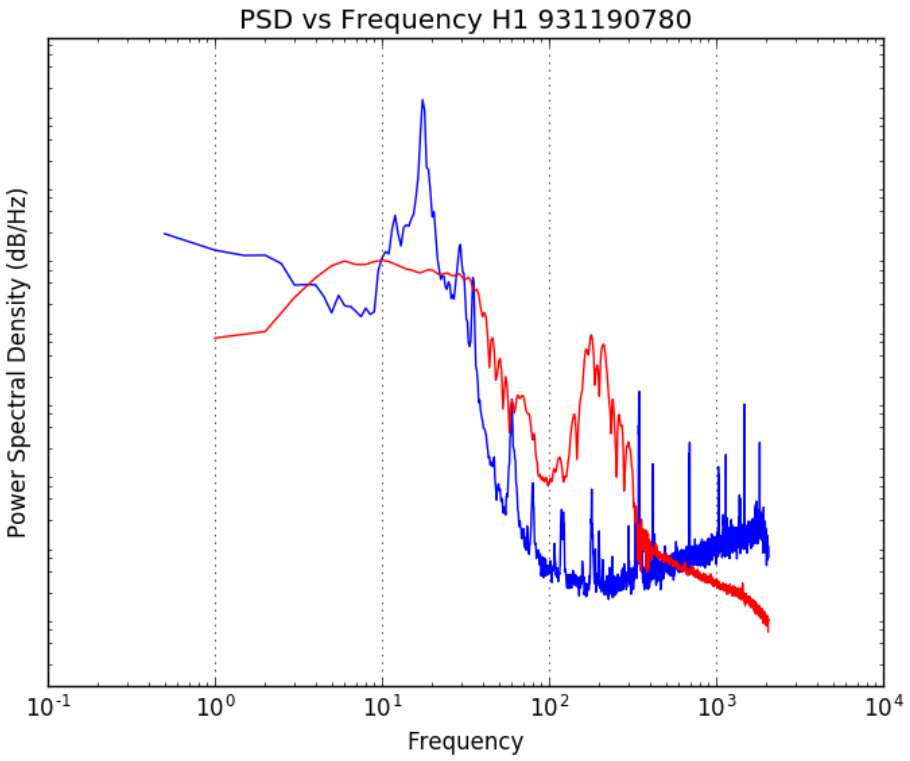

Figure 4: A plot of the power spectral density for the raw strain in blue and the template in red

This range was chosen because the power spectral density, which measures the intensity of a waveform as a function of frequency, of the template is stronger than the raw strain data. For frequency ranges in which the intensity of the template is much less than that of the raw strain, an SNR calculation would be irrelevant because any signal would be out of the LIGO detector's range of frequency detection. Thus the efficiency of the overall procedure is increased further, as some data is sorted out and considered not worthwhile to analyze. The bandpass filter is implemented using methods from the scipy python library.

The fourth phase of the analysis involves the template and employs time domain cross-correlation. This process takes into account both the raw strain and the template and finds where the greatest waveform match occurs in the specified time interval between the raw stain the template. The process is defined as follows [4]:

$$(s * h) = \int_{-\infty}^{\infty} s^*(t)h(t+\tau)dt \qquad (2)$$

Where s denotes the detector output, h denotes the template strain, s* denotes the complex conjugate of the output, and τ is the time lag associated with the difference between the total

time of the strain segment and the template. The template usually ranges in time between five and one hundred seconds, while the strain segments can run as long as 2048 seconds. In this case the strain is no longer the original strain because it previously went through the bandpass filter. Rather, it is filtered between 20 Hz and 250 Hz. A graph of the time domain cross-correlation demonstrates where in time greatest match begins with a large spike in the graph, an example of which is shown below in Figure 5.

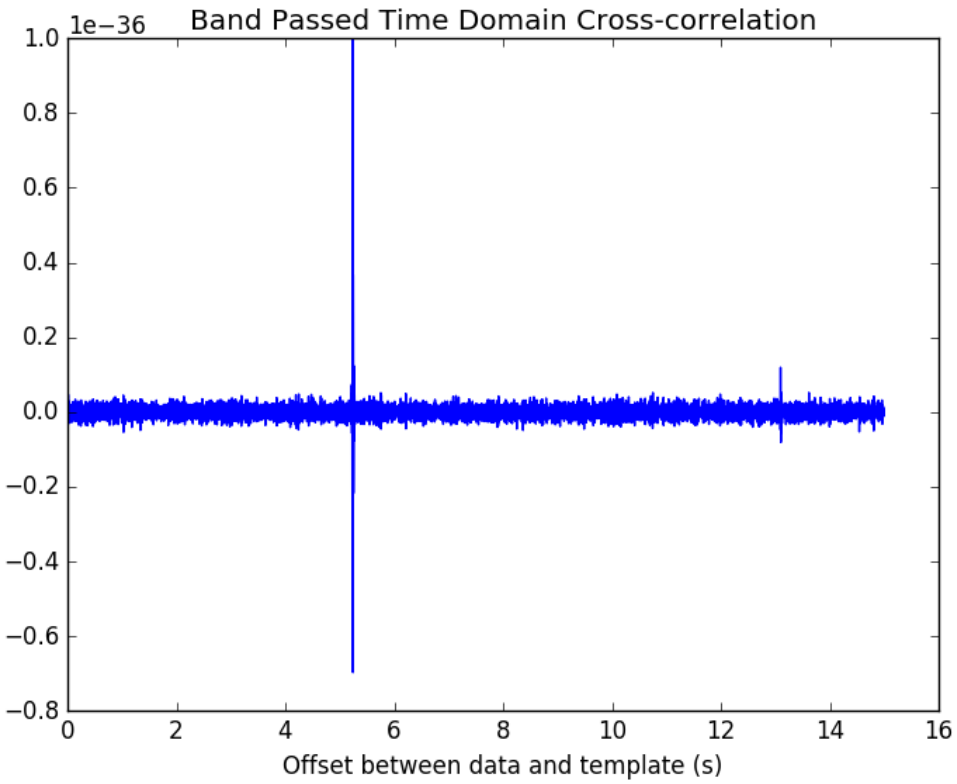

Figure 5: An example plot of time domain cross-correlation. The spike is where the greatest match between the strain and the template begins.

The fifth step in the main analysis process is to calculate the SNR of the template to the strain. The SNR is calculated from two quantities: the matched filter output and the normalization constant. The matched filter output is defined as follows [9]:

$$z(t) = 4\int_0^\infty \frac{\tilde{s}(f)\tilde{h}(f)}{S_n(f)} e^{2\pi i f t} df \qquad (3)$$

In (2), $\tilde{s}(f)$ denotes the Fourier transform of the output of the detector, $\tilde{h}(f)$ denotes the Fourier transform of the filter, and $S_n(f)$denotes the power spectral density of the signal. The normalization constant is defined [9]:

$$\sigma_m = 4\int_0^\infty \frac{|\tilde{h}(f)|}{S_n(f)}\,df \qquad (4)$$

The final SNR is simply the quotient of the absolute value of (2) and (3) [9]:

$$\rho(t) = \frac{|z(t)|}{\sigma_m} \qquad (5)$$

Notice how the SNR in equation (4) is no longer a function of frequency but instead of time. Consequently, the SNR can be plotted as a function of time and peaks in the graph of SNR vs. time are recorded along with the times at which they occur. This is done for both detectors and the whole process again for each strain segment and for each template.

4. Results

The range of detectable black hole natural frequencies was calculated by finding the intersection of the 20 Hz and 7,000 Hz frequency lines given by equation (1) with the formula for the black hole's radius as a function of mass, or the Schwarzschild radius given by:

$$R_{Schwarz} = \frac{2GM}{c^2} \qquad (6)$$

The result is plotted in Figure 6. The lower end of the mass range was .1 solar masses, which is lower than any stellar mass black hole and was done for graphical completeness, and the upper intersection yields a maximum mass of approximately 900 solar masses and a radius of $5.17x10^6m$.

Analysis of the first four months of S6 data yielded on average 340 time matches between detectors per template. In the time that was allotted for the analysis, only 31 templates out of 302 could be used. This requires visual analysis of almost 18,000 times, all of which that time permitted to be viewed had a likeness similar to the following. At the GPS time of 931190780, or July 9, 2009 at 16:06 UTC, the graph of SNR vs. Time for the H1 (Hanford 1) detector appeared as shown in Figure 7.

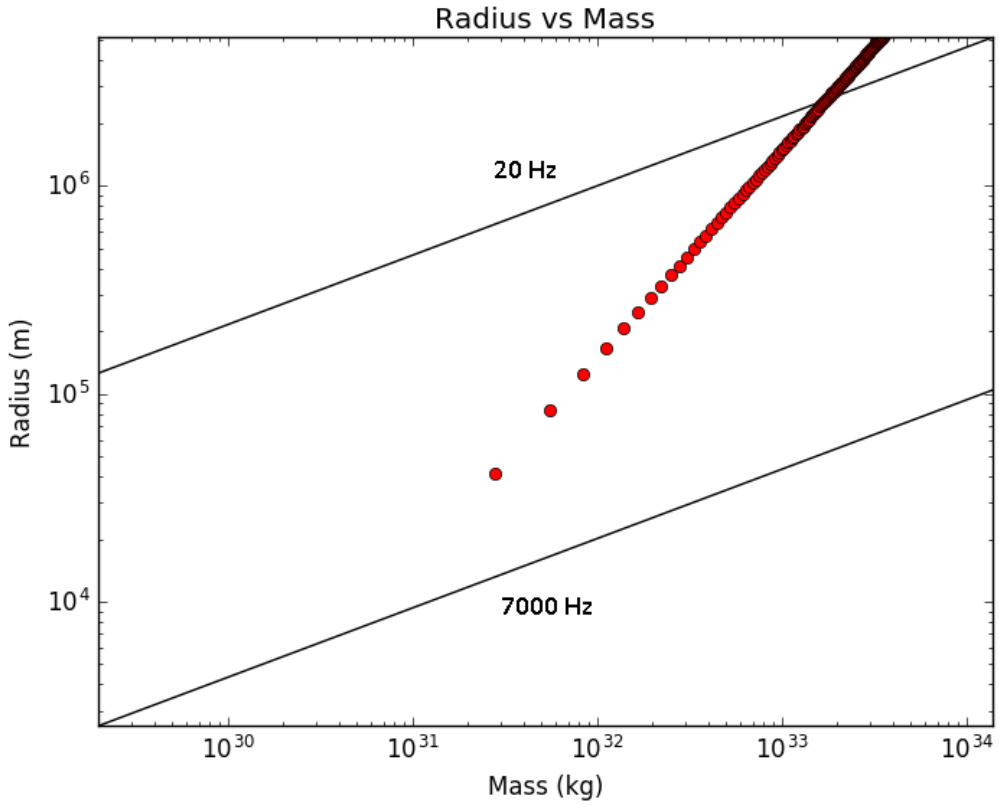

Figure 6: A plot of radius versus mass for a black hole. The upper solid line is the 20 Hz line and the lower solid line is the 7,000 Hz line.

The sharp peak in the graph of SNR vs. time in Figure 7 is when the signal became strong relative to the strain at its strongest time of correlation. In order to be a candidate for detection, the SNR must reach a peak within the allowed time window in the other detector. Indeed, Figure 8 demonstrates that the L1 detector experienced a maximum SNR within the time window. The very high SNR readings at the indicated time strongly suggest that the gravitational wave signal should be visible on the raw strain output plot. If a detection is made, then the high SNRs indicate that the signal power overwhelms the more or less random noise power. In addition, the signal should appear to be about the same on both detectors. Upon inspection in Figure 9, one can see that the raw strain plots are actually very dissimilar to each other. Here despite a high calculated SNR, the expected signal was not really there.

Hundreds of matching times that fell within the time window had a high SNR yet failed to register sufficient similarity in the raw strain profile to merit further consideration. A chart of

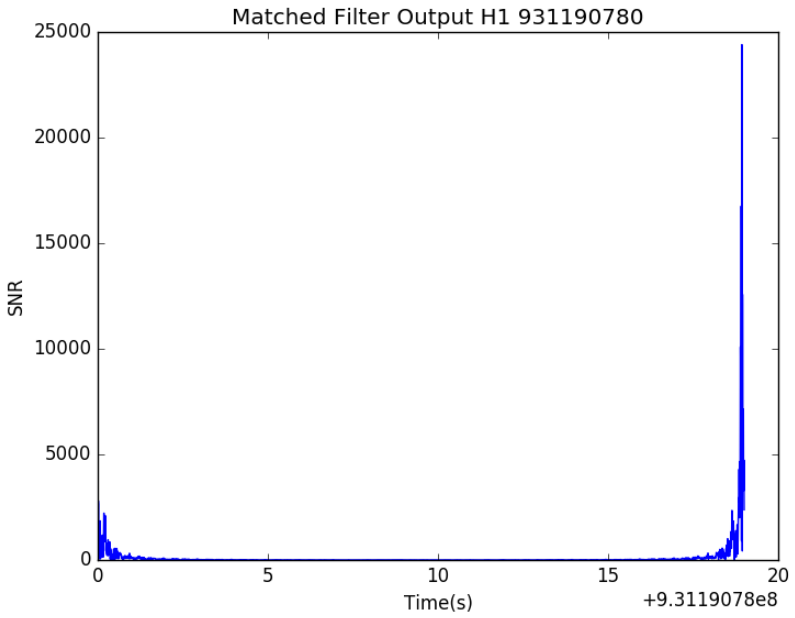

Figure 7: The plot of SNR vs. Time for the H1 detector and the SXS BBH 0001 template at GPS time 931190780. Notice the sharp peak in the graph that occurs 18 seconds after the start of the plot.

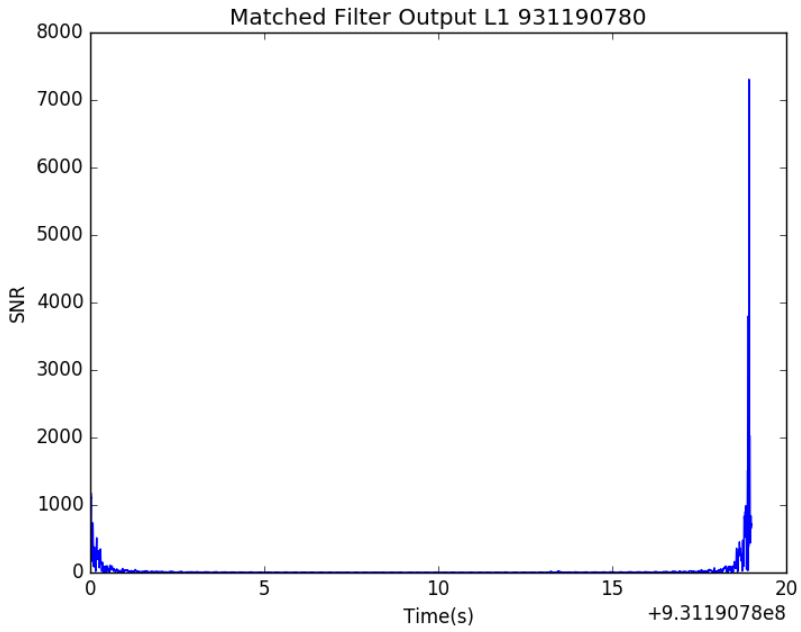

Figure 8: The plot of SNR vs. Time for the L1 detector and the SXS BBH 0001 template at GPS time 931190780. Notice the sharp peak in the graph that occurs around 18 seconds after the start of the plot.

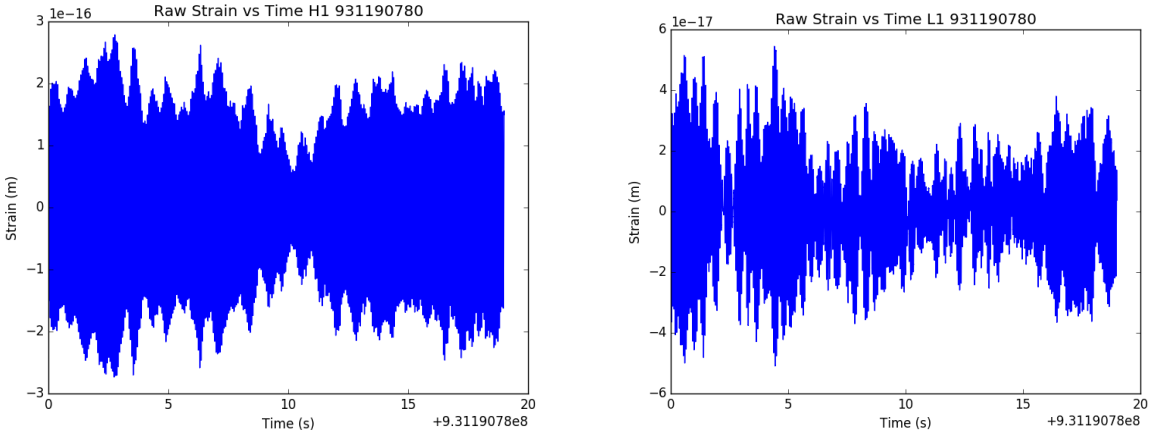

Figure 9: Plots of the raw strain data for both the H1 and L1 detectors around GPS time 931190780. The lack of obvious similarities between the two plots effectively rules out a gravitational wave detection.

the results is below:

	July 2009	August 2009	September 2009	October 2009
H1 SNRs > 8	6366	7709	2256	12597
L1 SNRs > 8	903	3062	1751	6412
Overlapping Times	63	47	21	335
Events worth further consideration	0	0	0	0

5. Discussion

The abundance of high SNR calculations suggests on the surface that there were many instances in which the template power, perhaps representing a gravitational wave signal, overwhelmed the noise power. The sheer number of times in which two high SNRs were observed within the allowed time window seemed to give further credence to the possibility that a gravitational wave detection was made. However, the results indicate that there is very little evidence for any such detections, as the SNRs are simply too large in most cases to substantiate a detection case from looking at the raw strain data.

The question regarding why the SNR values were so large only to come to nothing remains a valid one. One explanation is that the algorithm itself makes an overly optimistic appraisal of the SNR where the template corresponds most to the raw data. This goes back to the bandpass filtering step in which the raw strain data is restricted to frequencies at which the template is more intense. This was done with the intention of increasing computational efficiency. However, the bandpass filtered strain data may have been reduced to such an extent that the template was far more intense relative to the filtered strain than anticipated. Consequently, the calculated SNRs were much higher than expected for null results.

Another possibility for the high number or large SNR values is that the template models another phenomenon rather well. The fact that most high SNR values were unique to their detectors suggests that local phenomena that cause vibrations whose waveforms are inadvertently similar to the gravitational wave templates may have been the cause of these SNR values. This idea went untested because high SNR values unique to one detector were not examined in the raw strain. Once again, this decision was made to improve the efficiency of the search process.

6. Conclusions and Future Directions

This search and analysis did not find any gravitational wave candidates in the search space of the first four months of LIGO S6 data and only 31 out of hundred of numerical relativity templates. A wider search should be conducted in the future under more lenient time constraints. The remainder of the S6 data run should be analyzed, totaling an additional 12 months of data along with the hundreds of other templates. A more comprehensive search for gravitational wave sources should improve the prospects of detection. There is the possibility that no sources will be detected even with a more detailed search. This would mean that CBC events within the detectable range are rather rare and are truly special events.

More data from the Advanced LIGO configuration should be made publically available soon, which will enable the analysis of data that is on the order of 10 times as sensitive as data from LIGO S6 run. Indeed, two gravitational wave detections were confirmed by the Advanced LIGO team in late-2015, both of which were black hole CBC's. The increased sensitivity allows for the detection of black holes of a higher mass that emit gravitational waves of a lower frequency than the LIGO S6 configuration. In the coming decades, more sensitive gravitational

wave detectors will be constructed and implemented. Of particular interest is the planned space-based gravitational wave detector known as the Evolved Laser Interferometer Space Antenna or eLISA. Deemed a feasible project by the forerunner mission LISA Pathfinder in 2016, when eLISA comes online in the 2030's, it will be able to detect previously hidden gravitational wave sources. These include binary stars from within the Milky Way Galaxy, supermassive black holes in other galaxies, and perhaps waves from the early universe during the inflationary period [11]. The future holds bright prospects for the advancement of gravitational wave astronomy.

Bibliography

[1] LIGO Caltech (2006) https://www.ligo.caltech.edu/news/ligo20160211

[2] B.F. Schutz 2000 “Gravitational Wave Astronomy” *Arxiv*

[3] E.F. Taylor and J.A. Wheeler 2000 *Exploring Black Holes: Introduction to General Relativity* (Addison Wesley Longman, San Francisco).

[4] B.S. Sathyaprakash and B.F. Schutz 2009 “Physics, Astrophysics and Cosmology with Gravitational Waves” *Arxiv*

[5] Abbott, B. et al. (LIGO Scientific Collaboration), “Analysis of LIGO data for gravitational waves from binary neutron stars”, *Phys. Rev. D*, 69, 122001, (2004).

[6]European Space Agency
http://www.esa.int/Our_Activities/Space_Science/Herschel/How_many_stars_are_there_in_the_Universe.

[7] Abadie, J. et al. (LIGO Scientific Collaboration), “Predictions for the Rates of Compact Binary Coalescences Observable by Ground-based Gravitational-wave Detectors” arXiv:1003.2480v2 [astro-ph.HE]

[8] Kumar, P. et al. “Template Banks for Binary black hole searches with Numerical Relativity waveforms”, *Phys. Rev. D 89, 042002 (2014)*

[9] Wang, S. “Characterizations of Hardware Injections in LIGO Data”, *LIGO Surf 2014*, (2014).

[10] M.P. Norton and D.G. Karczub 2003 *Fundamentals of Noise and Vibration Analysis for Engineers* (Cambridge University Press, Cambridge)

[11] "Selected: The gravitational universe; ESA decides on next large mission concepts". eLISA Consortium. Retrieved 13 November 2016.